ISSN (Print) 0023-4001
ISSN (Online) 1738-0006

**Korean J Parasitol** Vol. 60, No. 3: 163-172, June 2022
https://doi.org/10.3347/kjp.2022.60.3.163

▣ ORIGINAL ARTICLE

# Kinesin-13, a Motor Protein, is Regulated by Polo-like Kinase in *Giardia lamblia*

Eun-Ah Park, Juri Kim, Mee Young Shin, Soon-Jung Park*

*Department of Environmental Medical Biology and Institute of Tropical Medicine, Yonsei University College of Medicine, Seoul 03722, Korea*

**Abstract:** Kinesin-13 (Kin-13), a depolymerizer of microtubule (MT), has been known to affect the length of *Giardia*. *Giardia* Kin-13 (GlKin-13) was localized to axoneme, flagellar tips, and centrosomes, where phosphorylated forms of *Giardia* polo-like kinase (GlPLK) were distributed. We observed the interaction between GlKin-13 and GlPLK via co-immunoprecipitation using transgenic *Giardia* cells expressing Myc-tagged GlKin-13, hemagglutinin-tagged GlPLK, and in vitro-synthesized GlKin-13 and GlPLK proteins. In vitro-synthesized GlPLK was demonstrated to auto-phosphorylate and phosphorylate GlKin-13 upon incubation with [γ-$^{32}$P]ATP. Morpholino-mediated depletion of both GlKin-13 and GlPLK caused an extension of flagella and a decreased volume of median bodies in *Giardia* trophozoites. Our results suggest that GlPLK plays a pertinent role in formation of flagella and median bodies by modulating MT depolymerizing activity of GlKin-13.

Key words: *Giardia lamblia*, GlKin-13, GlPLK, flagella, median body

## INTRODUCTION

*Giardia lamblia*, a pathogen causing gastrointestinal diseases in humans [1], is a unicellular organism with a polarity in which 2 nuclei, an adhesive disc, a median body, and 4 pairs of flagella are present in specific intracellular positions [2]. Correct positioning of these organelles is a critical step in cell division of *G. lamblia* in which microtubules (MTs) play an important role like other eukaryotic cells [3]. The growth and shrinkage of MTs should be finely modulated according to the phases of *Giardia* cell cycle.

Polymerization of MTs is mediated by MT-associated proteins called plus-end tracking proteins (+TIPs) that preferentially bind to the growing ends of polymerized MTs [4]. A +TIP studied in *Giardia* was *G. lamblia* end binding 1 (GlEB1) protein, which was found in the flagellar tips, median bodies, mitotic spindles, and nuclear membranes [5-7]. The function of GlEB1 in cell division was indirectly shown by the complementation assay using a microtubule-binding protein (*BIM1*) mutant of *Saccharomyces cerevisiae* [6], and also by anti-*gleb1* morpholino-mediated knockdown [7]. Through direct interaction with γ-tubulin, GlEB1 affects the MT nucleation activity of the γ-tubulin small complex (γ-TuSC), leading to defects in cytokinesis and flagella formation of *G. lamblia* [8]. In vitro-assays showed that GlEB1 exhibited MT binding activity in its dimeric form [7]. Interestingly, GlEB1 function during *Giardia* cell division is regulated by phosphorylation of the threonine #148 in GlEB1, which is mediated by *G. lamblia* aurora kinase (GlAK) [9].

In mammals, the activity of +TIPs is finely modulated by post-translational modifications; i.e., especially phosphorylation by aurora kinase (AK), polo-like kinase (PLK), and cyclin-dependent kinase (CDK). AK-mediated phosphorylation of highly expressed in cancer protein 1 (Hec1), a member of Nuclear division cycle 80 (Ndc80) complex at kinetochores, results in changes in affinity toward MTs [10]. Phosphorylation of cytoplasmic linker protein (CLIP)-170 and CLIP-associating proteins 2 by CDK1 recruits PLK1 to kinetochore, and PLK1-mediated phosphorylation of these +TIPs enhances CDK1 activity resulting in more stable kinetochore-MT attachment [11]. Phosphorylation of mitotic centromere-associated kinesin (MCAK) by AK causes in negative regulation of MT plus-end dynamic [12,13].

In *G. lamblia*, the role of GlAK in cytokinesis and flagella formation has been demonstrated using AK-specific inhibitors [9,14]. Of the *G. lamblia* CDKs [GlCDK1 (Accession no. XP_001704058.1; GL50803_8037) and GlCDK2 (Accession no. XP_001709931.1; GL50803_16802)], GlCDK1 forms a complex with

• Received 20 May 2022, revised 2 June 2022, accepted 3 June 2022.
* Corresponding author (sjpark615@yuhs.ac)

*G. lamblia* cyclin 3977 (Accession no. KWX12927.1; GL50803_3977), which shows kinase activity toward histone H1 [15]. On the other hand, GlCDK2 phosphorylates *G. lamblia* Myb2, a master transcription factor of encystation in *G. lamblia* [16]. A single GlPLK (Accession no. ESU43708.1; GL50803_104150) was demonstrated to play a role in cytokinesis and flagella biogenesis in studies using PLK inhibitors and morpholino-mediated knockdown [17]. The phosphorylated form of GlPLK was found in the basal bodies, cytoplasmic portion of anterior flagella, median bodies, and flagella tips in interphase cells whereas it was present at the mitotic spindles in dividing cells.

A major protein responsible for MT depolymerization is Kinesin-13, a non-progressive kinesin motor protein exists at both plus and minus ends of MTs [18]. A group of kinesin-13 proteins has an important role in specific events during mitosis, such as kinetochore-MT attachment. The other group functions in non-mitotic processes including flagella formation. A single GlKin-13 (Accession no. DQ395239; GL50803_16945) is present in *Giardia* database, which is co-localized with GlEB1 in *Giardia* trophozoites [5]. Ectopic expression of dominant-negative mutant GlKin-13 resulted in extension of flagella and decreased volume of median bodies at interphase, and defective mitotic spindles during cell division. Knockdown of *glkin-13* via CRISPR interference in *Giardia* cells confirmed the role of GlKin-13 as a MT depolymerase [19]. GlKin-13 is present at the same positions with phosphorylated form of GlPLK during interphase, which included flagella tips, median bodies, and cytoplasmic anterior axoneme [5,17]. In this study, we constructed transgenic *Giardia* trophozoites expressing hemagglutinin (HA)-tagged GlPLK and Myc-tagged GlKin-13. Interaction between GlPLK and GlKin-13 during flagella and median body formation was investigated to uncover the linking relationship between these 2 proteins in *G. lamblia*.

## MATERIALS AND METHODS

### *Giardia lamblia* cultivation

*G. lamblia* trophozoites (Strain WB, ATCC30957) (American Type Culture Collection, Manassas, Virgina, USA) were maintained in modified TYI-S33 medium (2% casein digest, 1% yeast extract, 1% glucose, 0.2% NaCl, 0.2% L-cysteine, 0.02% ascorbic acid, 0.2% $K_2HPO_4$, and 0.06% $KH_2PO_4$, pH 7.1) supplemented with 10% heat-inactivated calf serum (Sigma-Aldrich, St. Louis, Missouri, USA) and 0.5 mg/ml bovine bile at 37˚C [20]. The *Giardia* transfectants were grown in TYI-S-33 medium containing appropriate antibiotics at the following concentrations (50 µg/ml puromycin and 600 µg/ml G418).

### Antibody production

A 2,142 bp-long *glkin-13* DNA fragment was amplified by PCR using the primers, rKin-13-F and rKin-13-R (Supplementary Table S1), then cloned into the EcoRI/NotI sites of pET21b (Novagen, Madison, Wisconsin, USA) to produce pET-GlKin-13. Histidine-tagged GlKin-13 was induced in *Escherichia coli* BL21 (DE3) by adding 1 mM isopropyl-β-D-thioglactopyranoside at 37˚C. The resulting recombinant proteins were excised from the SDS-PAGE gels and used to immunize Sprague–Dawley rats (2 weeks old, female, as previously described) [21]. All animal experiments were approved by the institutional guidelines and the legal requirements (IACUC 2017-0015; approval number: 2012-0264-1).

### Western blot analysis

Cell extracts prepared from each experimental *Giardia* (cells without any plasmid, and cells carrying the HA-tagged GlPLK expression plasmid and Myc-tagged GlKin-13 expression plasmid) were separated by 6% SDS-PAGE under reducing condition and transferred to a polyvinylidene fluoride membrane (Millipore, Burlington, Massachusetts, USA). The blots were incubated with rat anti-GlKin-13 (1:1,000 dilution), mouse monoclonal anti-HA (1:1,000 dilution; Sigma-Aldrich), or mouse monoclonal anti-Myc (1:1,000 dilution; Santa Cruz Biotechnology, Dallas, Texas, USA) antibodies in Tris-buffered saline (TBST; 50 mM Tris–HCl) supplemented with 5% skim milk and 0.05% Tween 20) at 4˚C overnight. The membranes were further incubated with horseradish peroxidase-conjugated host-specific antibodies. The immunoreactive bands were visualized with an enhanced chemiluminescence system (Thermo Fisher Scientific, Waltham, Massachusetts, USA). Membranes probed with polyclonal rat antibodies against protein disulfide isomerase 1 (PDI1; Accession no. U64730.2; GL50803_29487) of *G. lamblia* (1:10,000 dilution) were used as loading controls [22].

### Immunocytochemistry

*Giardia* cells were applied to the poly-L-lysine coated glass slides for 10 min, fixed in ice-cold methanol at –20˚C for 10 min, and permeabilized with phosphate buffered saline (PBS; 137 mM NaCl, 2.7 mM KCl, 10 mM $Na_2HPO_4$, and 1.8 mM

$KH_2PO_4$, pH 7.4) with 0.5% Triton X-100 for 10 min. After blocking for 1 h in PBS/5% goat serum/3% bovine serum albumin, the cells were incubated with 1:100 diluted anti-GlKin-13 antibodies or anti-phosphorylated PLK (ab39068; Abcam, Cambridge, Massachusetts, USA) overnight at 4˚C, and subsequently incubated with 1:200 diluted Alexa Fluor 555-conjugated goat anti-rat IgG (Thermo Fisher Scientific). The slides were counterstained with diamidino-2-phenylindole (DAPI) and observed using an inverted confocal laser scanning microscope (LSM700; Carl Zeiss, Oberkochen, Germany).

### Construction of *G. lamblia* expressing HA epitope-tagged GlPLK and Myc epitope-tagged GlKin-13 proteins

A 2,184 bp-long DNA fragment encompassing the promoter region (150 bp) and open reading frame of the *glplk* gene was amplified from *Giardia* genomic DNA by PCR using Pplk-F and PLK-R (Supplementary Table S1). The resulting DNA fragment was cloned into the NotI and XhoI sites of pKS-3HA.neo [23] to obtain pGlPLK-HA.neo. A 2,292 bp-long DNA fragment encoding *glkin-13* was amplified using the primers Pkin-13-F and Kin-13-R and cloned into the NotI and ClaI sites of pKS-3Myc.pac [23] to generate pGlKin-13-Myc.pac. Expression fidelity of these constructs was verified by DNA sequencing.

### Transfection

Twenty micrograms of pGlPLK-HA.neo were transfected into $1 \times 10^7$ *Giardia* trophozoites by electroporation under the following conditions: 350 V, 1,000 μF, and 700 Ω (Bio-Rad, Hercules, California, USA). Transfectants were initially selected in TYI-S-33 medium containing G418 at 150 μg/ml, after which G418 concentrations were increased to 600 μg/ml. The expression of HA-tagged GlPLK was examined by Western blotting. *Giardia* trophozoites carrying pKS-3HA.neo were included as a control. Each of 5 sets of transfections were performed and 3 of which were examined for the expression of HA-tagged GlPLK.

A plasmid expressing Myc-epitope tagged GlKin-13 was also transfected into *Giardia* trophozoites, as described above. Transfectants were selected in TYI-S-33 medium containing 10 μg/ml puromycin, and the concentrations were increased to 50 μg/ml. Expression of Myc-tagged GlKin-13 was examined by Western blotting probed with anti-Myc antibodies.

### Co-immunoprecipitation

*Giardia* cells carrying pGlPLK-HA.neo and pGlKin-13-Myc.pac were harvested, washed 3 times with ice-cold PBS, and lysed with lysis buffer (10 mM Tris-Cl, 5 mM EDTA, 130 mM NaCl, and 1% Triton X-100, pH 7.4) containing protease inhibitor cocktail (GenDEPOT, Katy, Taxas, USA). Lysates precleared using Protein A/G Agarose (Thermo Fisher Scientific) for 1 h at 4˚C were incubated with monoclonal mouse anti-HA agarose beads (Sigma-Aldrich) or monoclonal mouse anti-Myc antibodies (Clontech, Mountain View, California, USA) at 4˚C overnight. Beads were washed with immunoprecipitation washing buffer (50 mM Tris-Cl, 150 mM NaCl, and 1% Triton X-100, pH 7.4) and resuspended in 2×SDS sample buffer. The samples were analyzed by Western blotting using anti-HA or anti-Myc antibodies.

### In vitro-transcription/translation of GlPLK and GlKin-13 proteins

A 2,037 bp-long DNA fragment of the *glplk* gene was amplified from *Giardia* genomic DNA by PCR using 2 primers, PLK-GBK-F and PLK-GBK-R (Supplementary Table S1) and cloned into the EcoRI and NotI sites of pGBK (Clontech) to obtain pGBK-PLK. A 2,142 bp-long DNA fragment encoding GlKin-13 was amplified using the primers, Kin13-GAD-F and Kin13-GAD-R, subsequently cloned into the EcoRI and XhoI sites of pGAD (Clontech) to generate pGAD-GlKin-13. The nucleotide sequences of these constructs were verified by DNA.

The TNT T7 Coupled Reticulocyte Lysate System (Promega, Madison, WI, USA) was used for the in vitro-synthesis of Myc-tagged GlPLK and HA-tagged GlKin-13. The DNA templates (0.5 μg each) were incubated with the transcription/translation mixture in 50 μl volume at 30˚C for 90 min. The synthesized protein products were analyzed by 6% SDS-PAGE and visualized by Western blotting probed with anti-HA or anti-Myc antibodies.

### Kinase assay

GlPLK and GlKin-13 were resuspended in 20 μl kinase buffer (50 mM Tris-HCl, 10% glycerol, 5 mM $MgCl_2$, 150 mM NaCl, 50 mM KCl, and 1 mM DTT, pH 8.0). The kinase assays were performed in the presence of 2.5 μCi [$\gamma$-$^{32}$P] ATP (3,000 Ci/mmol; BMS, Lawrence, New Jersey, USA). The kinase reactions were processed for 30 min at 30˚C, after which by the addition of SDS loading buffer. Samples were then subjected to 6% SDS-PAGE, dried, and autoradiographed.

### Morpholino-mediated knockdown

The expression of GlPLK and GlKin-13 was knocked down using morpholinos [24]. Specific morpholinos for GlPLK and GlKin-13 were designed from Gene Tools (Philomath, Oregon, USA) and their sequences are listed in Supplementary Table S1. Nonspecific oligomers were used as control morpholino. Cells ($5 \times 10^6$ in 0.3 ml medium) were treated with the lyophilized morpholino at a final concentration of 100 nM. After electroporation, the cells were grown for various timepoints up to 15 h and analyzed for GlPLK or GlKin-13 inhibition by Western blotting using anti-HA or anti-Myc antibodies. The cells at 15 h post-transfection were analyzed for flagella length and median body volume. Transfection was performed at least 5 times, and the data presented were derived from 3 independent experiments.

### Determination of flagella length

*Giardia* trophozoites ($1 \times 10^6$ cells/ml) treated with control or anti-*glplk*/anti-*glkin-13* morpholinos were stained with Giemsa. The cells were attached to slides, air-dried, and fixed in ice-cold 100% methanol for 10 min at 4˚C. They were then stained with 10% Giemsa solution for 40 min and washed with distilled water. The cells were observed under an Axiovert 200 microscope, and their differential interference contrast images were analyzed using FIJI [25]. The membrane-bound regions of the 4 types of flagella were measured using the line freehand tracing mode in ImageJ software (http://imagej.nih.gov/ij/). The flagella length was analyzed with 40 cells per experiment. Data are presented as the mean ± standard deviation (SD) of 3 independent experiments.

### Determination of median body volume of tubulin-labeled cells

*Giardia* cells treated with control or anti-*glkin-13*/anti-*glplk* morpholino were attached onto the glass slides, air-dried, and fixed with 100% methanol for 10 min. To measure the volume of the median bodies, the morpholino-treated cells were labeled with the monoclonal antibodies against α-tubulin (1:600 dilution; Sigma-Aldrich), followed by a reaction with AlexaFlour 488-conjugated ant-mouse IgG (1:200 dilution; Molecular Probes, Eugene, Oregon, USA). The immunofluorescence procedure was same as described above. Samples were observed with an LSM710 laser scanning confocal microscope (Carl Zeiss), and serial sections were acquired at 0.3 μm intervals. For the measurement of median body volume, image analysis was performed using Imaris (Bitplane, South Windsor, Colorado, USA).

### Statistical analysis

Data are presented as the meane ± SD of 3 independent experiments. Statistical analyses for pairwise comparisons were performed using Student's *t*-test. Differences with *P*-values $>0.05$ were considered statistically significant. $*P>0.05$; $**P>0.01$.

## RESULTS

### Localization of GlKin-13 in *Giardia* trophozoite cytoskeletal structures

To define the structures of *G. lamblia* localized by GlKin-13, antibodies targeted to recombinant GlKin-13 were generated. When *Giardia* extract was probed with these antibodies, a 78 kDa band of GlKin-13 protein was specifically recognized (Fig. 1A).

IFAs of *Giardia* trophozoites using these antibodies demonstrated labeling of basal bodies, and MT-containing structures such as axonemes and median body (Fig. 1B). In addition, red fluorescent spots were present at the ends of all 8 flagella tips.

### Localization of phosphorylated GlPLK in *Giardia* trophozoites

To determine localization of phosphorylated form of GlPLK, *Giardia* trophozoites were incubated with antibodies specific to phosphorylated PLK. As shown in Fig. 1C, IFA of interphase cells showed strong fluorescence at cytoplasmic axonemes of anterior flagella, flagellar tips, and median bodies. Basal bodies were also positively stained.

### Interaction between GlKin-13 and GlPLK

The activity of Kin-13 orthologues is known to be modulated according to its phosphorylation status by kinases [26]. The similar localization pattern of GlPLK and GlKin-13 led us to examine a possibility that GlPLK is responsible for modulation of GlKin-13 activity. Most of all, the plasmid expressing GlPLK was transfected into *Giardia* trophozoites, after which the cells were double transfected with another plasmid expressing GlKin-13. Expression of these 2 proteins was evidenced by Western blotting, while *Giardia* cells carrying empty vectors did not demonstrate any immunoreactive signal (Fig. 2A).

Extracts were prepared from the *Giardia* cells expressing co-

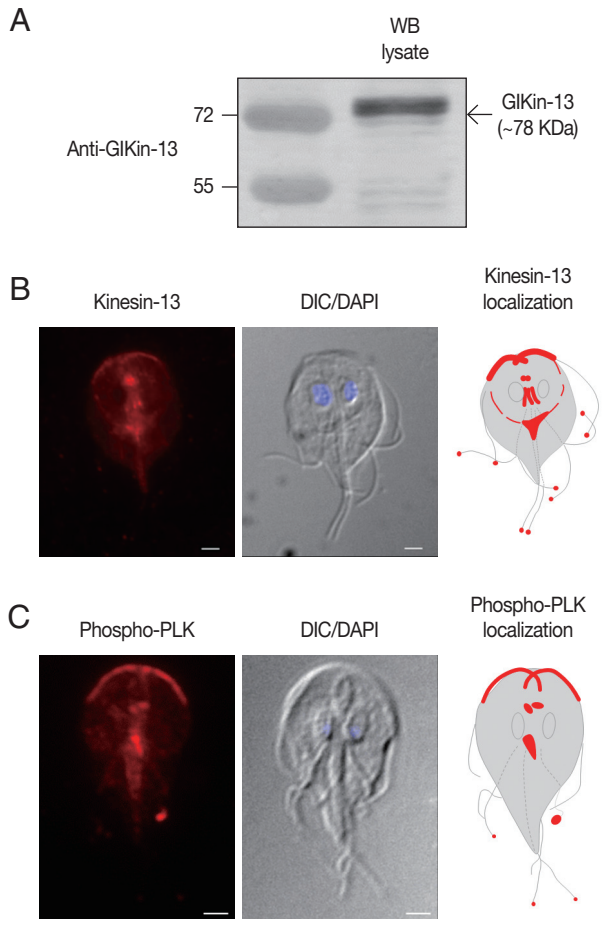


**Fig. 1.** Expression and localization of GlKin-13 and GlPLK in *G. lamblia*. (A) Western blotting to examine the specificity of anti-GlKin-13 antibodies. Extracts prepared from *G. lamblia* trophozoites, were incubated with rat anti-GlKin-13 antibodies. (B) An immunofluorescence assay showing localization of GlKin-13 in *Giardia* trophozoites. The cells were reacted with rat anti-GlKin-13 antibodies, and then Alexa Fluor 555-conjugated anti-rat IgG. (C) An immunofluorescence assay showing localization of phosphorylated GlPLK in *Giardia* trophozoites. The cells were reacted with rat anti-phosphorylated PLK antibodies, and then Alexa Fluor 555-conjugated anti-rat IgG. Slides were mounted with Gold Antifade Mountant with DAPI, and then examined with a Zeiss LSM700 inverted confocal laser scanning microscope. A differential interference contrast image was acquired to show cell morphology. Scale bars: 2 μm.

transfected HA-tagged GlPLK with Myc-tagged GlKin-13. The GlKin-13 protein was present in the immunoprecipitates prepared using anti-HA and was absent in those prepared using control IgG (Fig. 2B). Additionally, we performed a reciprocal immunoprecipitation using the anti-Myc antibody to immunoprecipitate GlKin-13 and then used Western blotting to determine if GlPLK co-precipitates. Fig. 2C shows that GlPLK is present in the anti-Myc immunoprecipitations, confirming the interaction (Fig. 2C).

To assess the interaction between GlKin-13 and GlPLK, the 2 separately synthesized [$^{35}$S]-methionine-labeled proteins were mixed and incubated. The mixtures were then immunoprecipitated with anti-Myc or anti-HA antibodies and resolved by SDS-PAGE. As shown in Fig. 2D, GlKin-13 was coprecipitated with GlPLK (lane 1 and 2) and vice versa (lane 3 and 4).

In vitro-synthesized GlPLK demonstrated auto-phosphorylation activity in the presence of [γ-$^{32}$P]ATP whereas incubation of GlKin-13 alone did not produce any radio-labeled protein (Fig. 3). Kinase assays including both GlPLK and GlKin-13 resulted in radio-labeling of both proteins, which demonstrated that GlPLK is able to undergo autophosphorylation, then transfer phosphate to GlKin-13.

### Role of GlPLK/GlKin-13 in formation of flagella and median body in *G. lamblia*

To define the role of GlPLK-mediated phosphorylation of GlKin-13 in *G. lamblia*, we designed anti-*glkin-13* morpholino to block the translation of *glkin-13* mRNAs (Supplementary Table S1) in addition to anti-*glplk* morpholino. These morpholinos were transfected into *Giardia* cells expressing GlPLK and GlKin-13. A control morpholino was also transfected into the same *G. lamblia* trophozoites. We analyzed expression patterns of cellular GlPLK and GlKin-13 15 h after transfection. Transfected cells suppressed expression of GlPLK and GlKin-13 by up to 47.8% and 59.0% compared to control morpholino-transfected cells (Fig. 4A).

The role of these proteins in flagella formation was further examined in GlPLK- and GlKin-13-depleted *Giardia*. As shown in Fig. 4B, GlPLK- and GlKin-13-defective cells demonstrated extension of 3 pairs of flagella compared with control morpholino-treated cells. However, the length of posterolateral flagella was not statistically different between cells treated with anti-*glkin-13* and anti-*glplk* morpholinos and those treated with control morpholino. The pronounced extension was observed in caudal and anterior flagella than ventral flagella in GlPLK- and GlKin-13-depleted cells.

Depletion of GlPLK and GlKin-13 also affected morphological features of median body, a MT-containing dynamic structure uniquely present in *Giardia* (Fig. 4C). We immunostained the cells against anti-α-tubulin antibodies and measured volume of median bodies. GlPLK and GlKin-13 knockdown cells showed decreased size of median bodies compared with that of control cells.

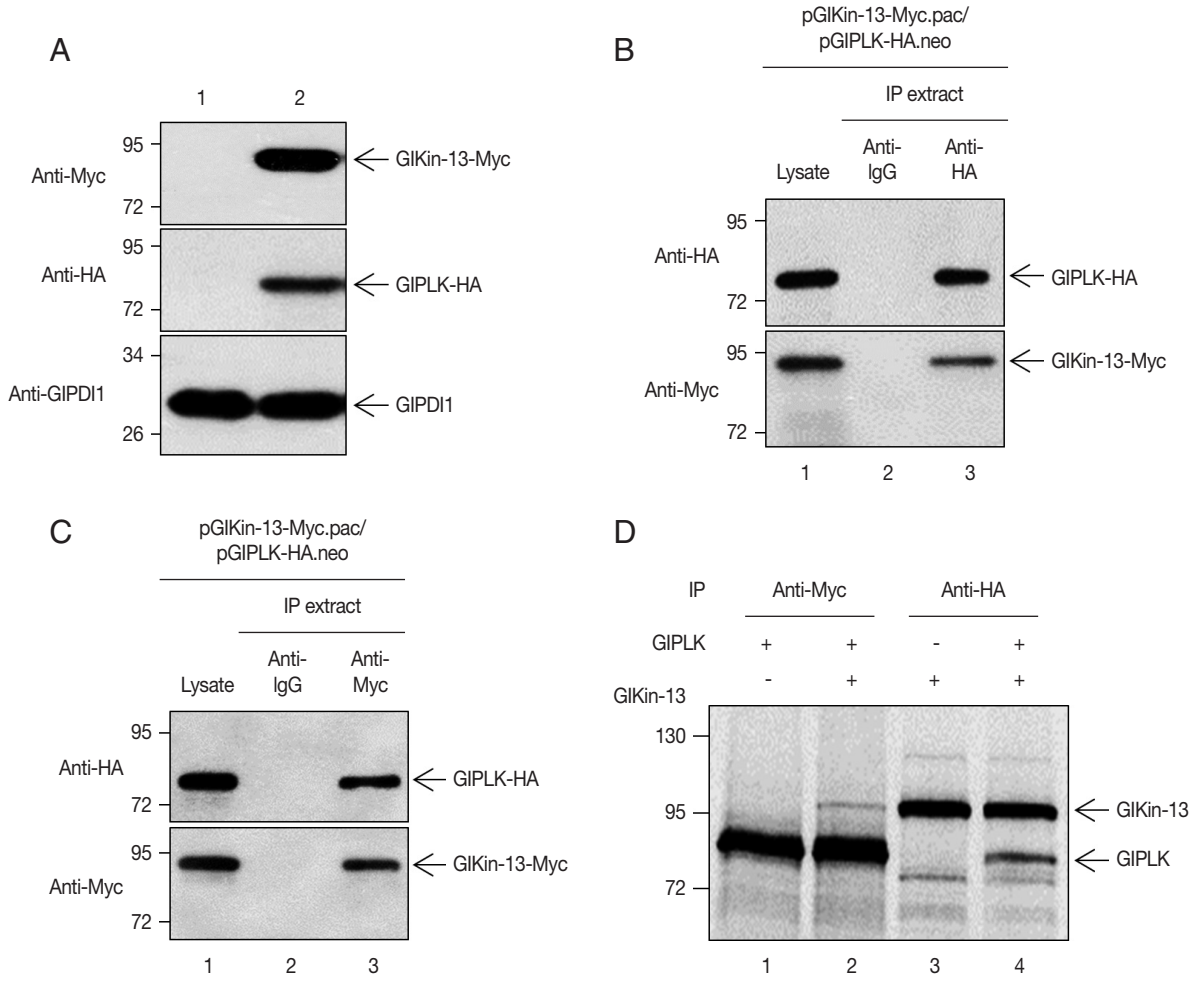


**Fig. 2.** Co-immunoprecipitation of GlKin-13 with GlPLK in *Giardia* ectopically expressing GlPLK and GlKin-13. (A) *Giardia* cells expressing Myc-tagged GlKin-13 and HA-tagged GlPLK were constructed. The expression of Myc-tagged GlKin-13 and HA-tagged GlPLK in these cells was demonstrated by Western blotting (lane 2). The cells carrying empty vectors were included as control (lane 1). (B, C) *Giardia* cells expressing Myc-tagged GlKin-13 and HA-tagged GlPLK were incubated with either anti-HA IgG agarose beads (B) or anti-Myc antibodies (C), and the resulting precipitates (lane 3) were analyzed by western blots using anti-HA or anti-Myc antibodies. As controls, the same *Giardia* lysates were included without any treatment (lane 1) or incubated with normal mouse IgG (lane 2) (D) Co-immunoprecipitation of GlPLK with GlKin-13. HA-tagged GlKin-13 and Myc-tagged GlPLK were expressed in vitro as labeled forms with [$^{35}$S]-methionine. Lane 1, Myc-tagged GlPLK precipitated with anti-Myc antibodies; lane 3, HA-tagged GlKin-13 sedimented with anti-HA antibodies; lanes 2 and 4, HA-tagged GlKin-13 and Myc-tagged GlPLK were mixed and incubated with either anti-Myc or anti-HA antibodies (lane 2 and 4, respectively). In vitro-synthesized GlKin-13 and GlPLK are indicated by arrows.

## DISCUSSION

While most other kinesins use their motor domain to move along MTs, kinesin-13 family members employ their ATP-hydrolyzing motor domain to destabilize MT ends. Human major kinesin-13s, Kinesin superfamily protein 2a (Kif2a), Kif2b, Kif2c, and Kif24 have been studied to understand their roles in mitosis as well as non-mitotic functions [27]. The Kif2c, also known as mitotic centromere associate kinesin (MCAK), has been extensively investigated [26]. Interestingly, 5 kinesin-13 proteins are present in *Trypanosoma brucei*, which have elaborate structures such as subpellicular MTs, intranuclear mitotic spindle, and flagella. Among them, nuclear-localized TbKif13-1 was identified as MCAK, and inhibition of TbKif13-1 function by RNA interference depletion resulted in defects in mitotic spindle formation [28]. TbKif13-2 was enriched in flagellar tip of *T. brucei* procyclic form [29] which was consistent with the function of the orthologous protein in *Leishmania major*, LmjKIN13-2 [30]. Another subset of kinesin-13 proteins is largely found in *Chlamydomonas*. These pro-

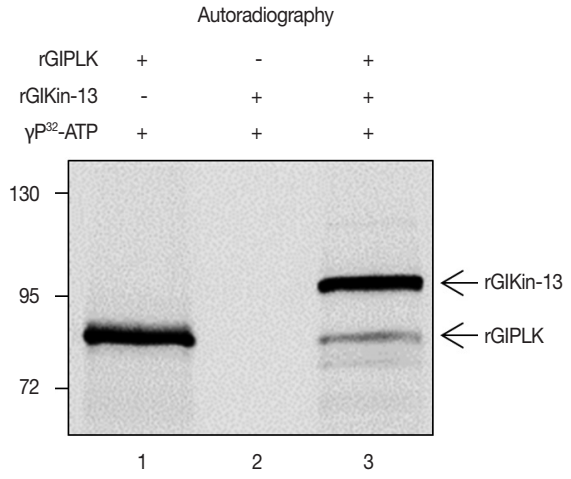


**Fig. 3.** Kinase activity of GlPLK against GlKin-13. Three micrograms of rGlPLK or rGlKin-13 was incubated with [γ-$^{32}$P]ATP (lanes 1 and 2, respectively). In lane 3, both rGlPLK and rGlKin-13 were included in the kinase reaction. The phosphorylated protein (s) was detected by autoradiography. In vitro-synthesized GlKin-13 and GlPLK are indicated by arrows.

teins were shown to be involved in flagella or cilia formation [31]. In *Tetrahymena thermophila*, a kinesin-13 had a mitotic function, while 2 other orthologs acted on the cell body and cilia. Loss of these non-mitotic kinesin-13s has resulted in overgrowth of cell body MTs and shortening of cilia. These results indicate that these kinesins may serve not only as MT depolymerase, but also as axoneme assemblers in a more complicated ways [32]. Only a single species of kinesin-13 is present in *Giardia* database, of which roles in mitosis and flagella length control had been demonstrated [5]. In addition, GlKin-13 is involved in MT equilibrium of median body, a unique structure of *G. lamblia*. Among the diverse functions of GlKin-13, this study focused on its non-mitotic roles by observing only the interphase cells, but not the dividing cells (Figs. 1, 2, 4).

In mammals, MCAK is recruited to the + end of MT via interaction with +TIP such as EB1 to act as a MT depolymerase [33]. This interaction is finely modulated by phosphorylation status of kinesin-13 through diverse cell cycle-related kinases. Phosphorylation of various residues of MCAK with aurora kinase A (AKA), aurora kinase B (AKB), or cyclin-dependent kinase 1 (CDK1) inhibits MT depolymerase activity, otherwise interfering with the interaction with +TIPs [12,13,34,35]. However, the action of PLK1 triggers a stimulatory effect on MCAK activity [36]. Localization pattern of GlKin-13 was the same as that of phosphorylated form of GlPLK, which are present in cytoplasmic portion of anterior flagella, flagellar tips, and median body of interphase cells (Fig. 1B, C). These results suggest a possibility that GlKin-13 activity is regulated by GlPLK-mediated phosphorylation. Our study also demonstrated that GlKin-13 and GlPLK interact (Fig. 2), in which GlKin-13 is a substrate of GlPLK (Fig. 3). The mammalian PLK1 activated MCAK [37]. Fluorescence resonance energy transfer-base reporter and quantitative analysis of native PLK1 substrate phosphorylation indicate that AKB phosphorylates PLK1 on threonine #210, which then transfers phosphate to serine #715 of MCAK, a key regulator for kinetochore-MT attachment [38]. Interaction of GlEB1 and GlKin-13 was also expected from their localization pattern at cytoplasmic anterior axoneme, flagellar tips, and median body in interphase cells and mitotic spindles in dividing cells [5]. MT depolymerization by GlKin-13 should be reconstituted in vitro to evaluate the functions of GlPLK and GlAK in this process.

Function of the GlPLK-GlKin-13 interaction in flagella and median body formation was examined in *Giardia* interphase cells, in which the expression of both components was depleted (Fig. 4B, C). Depletion of these components resulted in extension of only 3 pairs of caudal, anterior, and ventral flagella. The length of caudal and anterior flagella was especially affected compared to ventral flagella. Among the 4 pairs of *Giardia* flagella, posterolateral and ventral flagella are newly synthesized while caudal and anterior flagella are derived from mother cells during cell division [39]. Thus, knockdown of the MT-nucleating center, γ-TuSC components, including γ-tubulin preferentially affected newly synthesized flagella [8]. Since GlKin-13 functions as a MT depolymerase, its depletion may have profound effects on pre-existing and inherited flagella. Depletion of GlKin-13 and GlPLK caused decrease in median body size of interphase cells (Fig. 4C) as previously observed in GlKin-13-depleted cells [5]. Failure to recycle tubulin resulted in the lower depolymerase activity of GlKin-13 and that produces *Giardia* cells with smaller median body due to lack of tubulin storage.

In conclusion, the same intracellular localization of GlKin-13 with phosphorylated GlPLK in interphase *Giardia* cells led us to demonstrate the interaction and kinase activity of GlPLK against GlKin-13. This study shows that a small portion in complex reaction cascades of MT dynamics in *G. lamblia* is comprised of GlPLK, GlKin-13, and MT dynamics during interphase phenotypes, and the flagella and median body formation (Fig. 5).

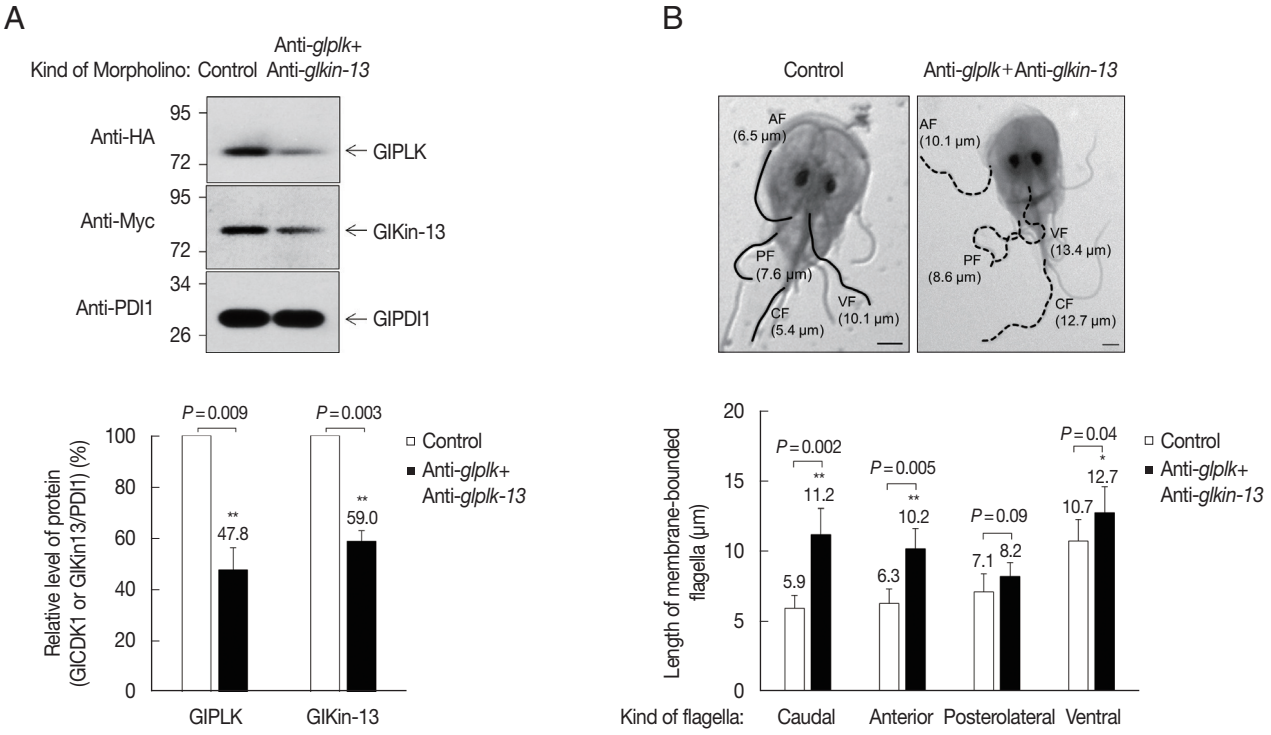


**Fig. 4.** Effect of morpholino-mediated GlPLK and GlKin-13 depletion in flagella and median body formation in *G. lamblia*. *Giardia* trophozoites expressing HA-tagged GlPLK and Myc-tagged GlKin-13 were collected at 15 h after electroporation with control or mixture of anti-*glplk* and anti-*glkin-13* morpholinos. (A) Morpholino-mediated GlPLK and GlKin-13 knockdown *G. lamblia* shown by Western blot analysis using anti-HA or anti-Myc antibodies (upper panel). The relative expression of HA-tagged GlPLK and Myc-tagged GlKIn-13 in extracts of cells treated with anti-*glplk* and anti-*glkin-13* morpholinos compared with those in the control cells is presented as a bar graph (lower panel). $^{**}P<0.01$. (B) Effects of morpholino-mediated GlPLK and GlKin-13 depletion on the flagella length of *G. lamblia*. The cells transfected with control (open bars) or mixture of anti-*glplk* and anti-*glkin-13* morpholinos (closed bars) were maintained for 15 h prior to staining with Giemsa solution. Representatives for the depleted cells and control cells are presented (upper panel). Forty cells were examined for flagella length (lower panel). Data are presented as an average of 3 independent experiments. $^{*}P<0.05$ and $^{**}P<0.01$. (C) Effect of morpholino-mediated knockdown of GlKin-13 and GlPLK on the volume of the median body. To measure the volume of median body, the cells were stained with anti-α-tubulin antibodies (1:600), followed by a reaction with AlexaFlour 488-conjugated anti-mouse IgG (1:200). The stained cells were observed using a Zeiss LSM710 laser scanning confocal microscope. Representatives for the depleted cells and control cells are presented (upper panel). For the measurement of median body volume, images were measured using the Imaris software. Arrow heads indicate the median bodies stained with α-tubulin antibody (lower panel). The significance of differences between the experimental conditions was evaluated by Student's t tests. $^{**}P<0.01$.

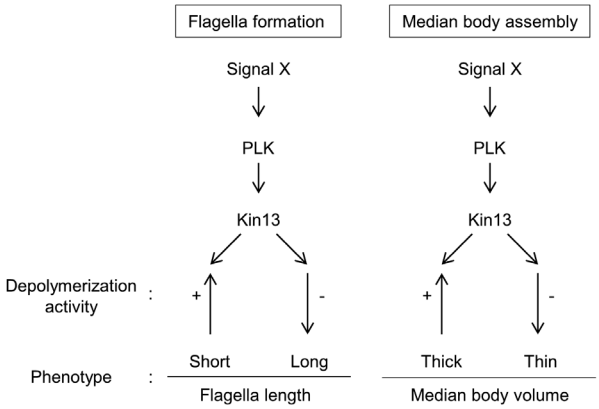


**Fig. 5.** A schematic diagram of the GlPLK-GlKin-13 signaling pathway involved in formation of flagella and median body in interphase *Giardia* cells.

## ACKNOWLEDGMENTS

This research was supported by Basic Science Research Program through the National Research Foundation of Korea (NRF) funded by the Korea government (MSIT) (NRF-2018 R1D1A1A02085338 to S-J. Park and NRF-2020R1C1C1010581 to J. Kim).

## CONFLICT OF INTEREST

The authors declare that they have no conflict of interest.

## REFERENCES

1. Nash TE. Unraveling how *Giardia* infections cause disease. J Clin Invest 2013; 123: 2346-2347. http://doi.org/10.1172/JCI69956
2. Elmendorf HG, Dawson SC, McCaffery JM. The cytoskeleton of *Giardia lamblia*. Int J Parasitol 2003; 33: 3-28. http://doi.org/10.1016/S0020-7519(02)00228-X
3. Desai A, Mitchison TJ. Microtubule polymerization dynamics. Ann Rev Cell Develop Biol 1997; 13: 83-117. http://doi.org/10.1146/annurev.cellbio.13.1.83
4. Akhmanova A, Steinmetz MO. Tracking the ends: a dynamic protein network controls the fate of microtubule tips. Nat Rev Mol Cell Biol 2008; 9: 309-322. http://doi.org/10.1038/nrm2369
5. Dawson SC, Sagolla MS, Mancuso JJ, Woessner DJ, House SA, Fritz-Laylin L, Cande WZ. Kinesin-13 regulates flagellar, interphase, and mitotic microtubule dynamics in *Giardia intestinalis*. Eukaryot Cell 2007; 6: 2354-2364. http://doi.org/10.1128/EC.00128-07
6. Kim J, Sim S, Kim J, Song K, Yong TS, Park SJ. *Giardia lamblia* EB1 is a functional homolog of yeast Bim1p that binds to microtubules. Parasitol Int 2008; 57: 465-471. http://doi.org/10.1016/j.parint.2008.05.008
7. Kim J, Nagami S, Lee KH, Park SJ. Characterization of microtubule-binding and dimerization activity of *Giardia lamblia* end-binding 1 protein. PLoS One 2014; 9: e97850. http://doi.org/10.1371/journal.pone.0097850
8. Kim J, Park SJ. Roles of end-binding 1 protein and gamma-tubulin small complex in cytokinesis and flagella formation of *Giardia lamblia*. Microbiologyopen 2019; 8: e00748. http://doi.org/10.1002/mbo3.748
9. Kim J, Lee HY, Lee KH, Park SJ. Phosphorylation of serine 148 in *Giardia lamblia* end-binding 1 protein is important for cell division. J Eukaryot Microbiol 2017; 64: 464-480. http://doi.org/10.1111/jeu.12384
10. Wimbish RT, DeLuca JG. Hec1/Ndc80 tail domain function at the kinetochore-microtubule interface. Front Cell Dev Biol 2020; 8: 43. http://doi.org/10.3389/fcell.2020.00043
11. Maia AR, Garcia Z, Kabeche L, Barisic M, Maffini S, Macedo-Ribeiro S, Cheeseman IM, Compton DA, Kaverina I, Maiato H. Cdk1 and Plk1 mediate a CLASP2 phospho-switch that stabilizes kinetochore–microtubule attachments. J Cell Biol 2012; 199: 285-301. http://doi.org/10.1083/jcb.201203091
12. Zhang X, Lan W, Ems-McClung SC, Stukenberg PT, Walczak CE. Aurora B phosphorylates multiple sites on mitotic centromere-associated kinesin to spatially and temporally regulate its function. Mol Biol Cell 2007; 18: 3264-3276. http://doi.org/10.1091/mbc.E07-01-0086
13. Zhang X, Ems-McClung SC, Walczak CE. Aurora A phosphorylates MCAK to control Ran-dependent spindle bipolarity. Mol Biol Cell 2008; 19: 2752-2765. http://doi.org/10.1091/mbc.E08-02-0198
14. Davids BJ, Williams S, Lauwaet T, Palanca T, Gillin FD. *Giardia lamblia* aurora kinase: a regulator of mitosis in a binucleate parasite. Int J Parasitol 2008; 38: 353-369. http://doi.org/10.1016/j.ijpara.2007.08.012
15. Gourguechon S, Holt LJ, Cande WZ. The *Giardia* cell cycle progresses independently of the anaphase-promoting complex. J Cell Sci 2013; 126: 2246-2255. http://doi.org/10.1242/jcs.121632
16. Cho CC, Su LH, Huang YC, Pan YJ, Sun CH. Regulation of a Myb transcription factor by cyclin-dependent kinase 2 in *Giardia lamblia*. J Biol Chem 2012; 287: 3733-3750. http://doi.org/10.1074/jbc.M111.298893
17. Park EA, Kim J, Shin MY, Park SJ. A polo-like kinase modulates cytokinesis and flagella biogenesis in *Giardia lamblia*. Parasite Vectors 2021; 14: 182. http://doi.org/10.1186/s13071-021-04687-5
18. Moores CA, Milligan RA. Visualisation of a kinesin-13 motor on microtubule end mimics. J Mol Biol 2008; 377: 647-654. http://doi.org/10.1016/j.jmb.2008.01.079
19. McInally SG, Hagen KD, Nosala C, Williams J, Nguyen K, Booker J, Jones K, Dawson SC. Robust and stable transcriptional repression in *Giardia* using CRISPRi. Mol Biol Cell 2019; 30: 119-130. http://doi.org/10.1091/mbc.E18-09-0605
20. Keister DB. Axenic culture of *Giardia lamblia* in TYI-S-33 medium supplemented with bile. Trans R Soc Trop Med Hyg 1983; 77: 487-488. http://doi.org/10.1016/0035-9203(83)90120-7

21. Kim J, Lee HY, Lee MA, Yong TS, Lee KH, Park SJ. Identification of α-11 giardin as a flagellar and surface component of *Giardia lamblia*. Exp Parasitol 2013; 135: 227-233. http://doi.org/10.1016/j.exppara.2013.07.010
22. Kim J, Shin MY, Park SJ. RNA-sequencing profiles of cell cycle-related genes upregulated during the G2-phase in *Giardia lamblia*. Korean J Parasitol 2019; 57: 185-189. http://doi.org/10.3347/kjp.2019.57.2.185
23. Gourguechon S, Cande WZ. Rapid tagging and integration of genes in *Giardia intestinalis*. Eukary Cell 2011; 10; 142-145. http://doi.org/10.1128/EC.00190-10
24. Carpenter ML, Cande WZ. Using morpholinos for gene knockdown in *Giardia intestinalis*. Eukaryot Cell 2009; 8: 916-919. http://doi.org/10.1128/EC.00041-09
25. Schindelin J, Arganda-Carreras I, Frise E, Kaynig V, Longair M, Pietzsch T, Preibisch S, Rueden C, Saalfeld S, Schmid B, Tinevez J, White DJ, Hartenstein V, Eliceiri K, Tomancak P, Cardona A. Fiji: an open source platform for biological image analysis. Nat Methods 2012; 9: 676-682. http://doi.org/10.1038/nmeth.2019
26. Tanenbaum ME, Medema RH, Akhmanova A. Regulation of localization and activity of the microtubule depolymerase MCAK. Bioarchitecture 2011; 1: 80-87. http://doi.org/10.4161/bioa.1.2.15807
27. Manning AL, Ganem NJ, Bakhoum SF, Wagenbach M, Wordeman L, Compton DA. The Kinesin-13 proteins Kif2a, Kif2b, and Kif2c/MCAK have distinct roles during mitosis in human cells. Mol Biol Cell 2007; 18: 2970-2979. http://doi.org/10.1091/mbc.E07-02-0110
28. Chan KY, Matthews KR, Ersfeld K. Functional characterisation and drug target validation of a mitotic kinesin-13 in *Trypanosoma brucei*. PLoS Pathog 2010; 6: e1001050. http://doi.org/10.1371/journal.ppat.1001050
29. Wickstead B, Carrington JT, Gluenz E, Gull K. The expanded kinesin-13 repertoire of *Trypanosomes* contains only one mitotic kinesin indicating multiple extra-nuclear roles. PLoS One 2010; 5: e15020. http://doi.org/10.1371/journal.pone.0015020
30. Blaineau C, Tessier M, Dubessay P, Tasse L, Crobu L, Pagès M, Bastien P. A novel microtubule–depolymerizing kinesin involved in length control of a eukaryotic flagellum. Curr Biol 2007; 17: 778-782. http://doi.org/10.1016/j.cub.2007.03.048
31. Piao T, Luo M, Wang L, Guo Y, Li D, Li P, Snell WJ, Pan J. A microtubule depolymerizing kinesin functions during both flagellar disassembly and flagellar assembly in *Chlamydomonas*. Proc Natl Acad Sci USA 2009; 106: 4713-4718. http://doi.org/10.1073/pnas.0808671106
32. Vasudevan KK, Jiang Y, Lechtreck KF, Kushida Y, Alford LM, Sale WS, Hennessey T, Gaertig J. Kinesin-13 regulates the quantity and quality of tubulin inside cilia. Mol Biol Cell 2015; 26: 478-494. http://doi.org/10.1091/mbc.E14-09-1354
33. Lee T, Langford KJ, Askham JM, Brüning-Richardson A, Morrison EE. MCAK associates with EB1. Oncogene 2008; 183: 1223-1333. https://doi.org/10.1038/sj.onc.1210867
34. Sanhaji M, Friel CT, Kreis N, Krämer A, Martin C, Howard J, Strebhardt K, Yuan J. Functional and spatial regulation of mitotic centromere-associated kinesin by cyclin-dependent kinase 1. Mol Cell Biol 2010; 30: 2594-2607. http://doi.org/10.1128/MCB.00098-10
35. Dragestein KA, van Cappellen WA, van Haren J, Tsibidis GD, Akhmanova A, Knoch TA, Grosveld F, Galjart N. Dynamic behavior of GFP–CLIP-170 reveals fast protein turnover on microtubule plus ends. J Cell Biol 2008; 180: 729-737. http://doi.org/10.1083/jcb.200707203
36. Sanhaji M, Ritter A, Belsham HR, Friel CT, Roth S, Louwen F, Yuan J. Polo-like kinase 1 regulates the stability of the mitotic centromere-associated kinesin in mitosis. Oncotarget 2014; 5: 3130-3144. http://doi.org/10.18632/oncotarget.1861
37. Ritter A, Sanhaji M, Steinhäuser K, Roth S, Louwen F, Yuan J. The activity regulation of the mitotic centromere-associated kinesin by Polo-like kinase 1. Oncotarget 2015; 6: 6641-6655. http://doi.org/10.18632/oncotarget.2843
38. Shao H, Huang Y, Zhang L, Yuan K, Chu Y, Dou Z, Jin C, Garcia-Barrio M, Liu X, Yao X. Spatiotemporal dynamics of Aurora B-PLK1-MCAK signaling axis orchestrates kinetochore bi-orientation and faithful chromosome segregation. Sci Rep 2015; 5: 12204. http://doi.org/10.1038/srep12204
39. Nohýnková E, Tumová P, Kulda J. Cell division of *Giardia intestinalis*: Flagellar developmental cycle involves transformation and exchange of flagella between mastigonts of a diplomonad cell. Eukaryotic Cell 2006; 5: 753-761. http://doi.org/10.1128/EC.5.4.753-761.2006